

The drip lines of kaonic nuclei

J. Guo, D. H. Chen, Xian-Rong Zhou,* and Q. B. Chen

Department of Physics, East China Normal University, Shanghai 200241, China

H.-J. Schulze

INFN Sezione di Catania, Dipartimento di Fisica, Università di Catania, Via Santa Sofia 64, 95123 Catania, Italy

(Dated: May 18, 2021)

The effects of an additional K^- meson on the neutron and proton drip lines are investigated within Skyrme-Hartree-Fock approach combined with a Skyrme-type kaon-nucleon interaction. While an extension of the proton drip line is observed due to the strongly attractive K^-p interaction, contrasting effects (extension and reduction) on the neutron drip line of Be, O, and Ne isotopes are found. The origin of these differences is attributed to the behavior of the highest-occupied neutron single-particle levels near the neutron drip line.

I. INTRODUCTION

Kaonic nuclei, bound states of a negatively-charged kaon K^- and a normal nucleus, can provide valuable information concerning the kaon-nucleon interactions at low energies. Since Kishimoto suggested in 1999 the existence of K^- nuclei with a medium atomic number based on the strong attraction in the K^-N system [1], and Akaishi and Yamazaki discussed the possibility of K^- nuclei in few-body systems in 2002 [2], K^- nuclei have become one of the important problems that attracted significant attention from both experimental and theoretical sides in the study of strangeness physics.

In the past fifteen years, the properties of K^- nuclei have been studied actively in several experiments. For example, in 2005 the FINUDA collaboration succeeded to detect a kaon-bound state K^-pp through its two-body decay into a Λ hyperon and a proton and determined the corresponding binding energy and decay width [3]. Later on in 2010, a deeply bound and compact K^-pp state formed in the $pp \rightarrow K^+ + K^-pp$ reaction was found by analyzing the data of the DISTO experiment on the exclusive $pp \rightarrow p\Lambda K^+$ reaction [4]. Its mass and width were also obtained. Recently, the bound state K^-pp was detected by the E15 and E27 collaborations at J-PARC. The E15 collaboration found a bound state K^-pp with a binding energy of $47 \pm 3_{-6}^{+3}$ MeV [5]. The E27 collaboration observed a deeply bound state K^-pp produced by the reaction $\pi^+ + n + p \rightarrow K^-pp + K^+ \rightarrow \Sigma^0 + p + K^+$ [6]. As is noted, the main focus of current experiments is on the simplest kaonic nucleus K^-pp ; thus searching for new kaonic nuclei in the future is necessary, and of course, can open up lots of new opportunities for theoretical studies.

On the theoretical side, various models were used to study the properties of K^- nuclei. For example, the antisymmetrized molecular dynamics model [7], the effective chiral Lagrangian for the kaon-baryon interaction combined with a nonrelativistic baryon-baryon interaction model [8], the chiral SU(3) model [9], the chiral meson-baryon coupled-channels interaction models [10], the non-relativistic Faddeev and Faddeev-Yakubovsky calculations [11, 12]. For the density functional theory, several relativistic mean field (RMF)

models explored many properties of light K^- nuclei, such as level inversion, binding energy, decay widths, and density distributions [13–17]. Within Skyrme-Hartree-Fock (SHF) model, we studied the potential energy surfaces, mean fields, and the density distributions of K^- nuclei for various effective K^-N interaction strengths [18, 19].

One notes that these pioneering works focussed mainly on the kaon removal energy and width. However, a general understanding of strange nuclear systems requires the evaluation of the global strange nuclear chart, with strangeness as the third dimension. In particular, the location of the nuclear drip lines is an important information to understand the limits of the strong force to hold together the nucleons in a bound system. There are many studies concerning the drip lines in normal nuclear systems, but much less works regarding strangeness. For example, for the Λ [20–31], Σ [20, 32–35], and Ξ [20, 36–40] hypernuclei, the potentials, single-hyperon levels, deformation, density distributions, and binding energies have been investigated extensively. But only for Λ hypernuclei the neutron drip lines were investigated, e.g., in Refs. [41–43]. Definitely, the prediction of the drip lines in K^- nuclei is of importance to explore the strange nuclear chart in the future.

Therefore, the present work aims to provide the first investigation of the effects of an additional K^- on the neutron and proton drip lines in some typical K^- nuclei within the SHF approach. We take the isotopes of the typical nuclei Be, O, and Ne as examples. While most of Be and Ne isotopes are deformed, the deformations of O isotopes are very small.

The paper is organized as follows. In Sec. II, the extended SHF approach as well as the Skyrme-type K^-N force are introduced. In Sec. III, the energies of the highest-occupied single-particle levels, one-nucleon separation energies, binding energies, and quadrupole deformations of K^- nuclei in Be, O, and Ne isotopes are presented together with the corresponding normal nuclei and the available experimental data. Finally, a summary is given in Sec. IV.

II. THEORETICAL FRAMEWORK

The main purpose of the present work is to discuss the effect of an additional K^- meson on the neutron and proton drip

arXiv:2105.07735v1 [nucl-th] 17 May 2021

* xrzhou@phy.ecnu.edu.cn

lines in the SHF approach combined with a simple density-dependent Skyrme-type K^-N interaction. In this approach the total energy of the nucleus can be expressed as [18, 19, 44–50]

$$E = \int d^3r \varepsilon(\mathbf{r}), \quad \varepsilon = \varepsilon_{NN} + \varepsilon_{KN} + \varepsilon_C, \quad (1)$$

where ε_{NN} denotes the energy density of the nucleon-nucleon part, ε_{KN} is the energy density due to the kaon-nucleon interaction, and ε_C is the Coulomb contribution of protons and kaons.

For each single-particle (s.p.) state ϕ_q^i ($q = n, p, K$), the minimization of the total energy E in Eq. (1) implies the SHF Schrödinger equation

$$\left[-\nabla \cdot \frac{1}{2m_q^*} \nabla + V_q(\mathbf{r}) - \mathbf{W}_q(\mathbf{r}) \cdot (\nabla \times \boldsymbol{\sigma}) \right] \phi_q^i(\mathbf{r}) = e_q^i \phi_q^i(\mathbf{r}), \quad (2)$$

with the mean fields

$$V_K = \frac{\partial \varepsilon_{KN}}{\partial \rho_K} - V_C, \quad (3)$$

$$V_q = V_q^{\text{SHF}} + V_q^{(K)}, \quad V_q^{(K)} = \frac{\partial \varepsilon_{KN}}{\partial \rho_q}, \quad (q = n, p), \quad (4)$$

where V_C denotes the Coulomb field, V_q^{SHF} the standard nucleonic Skyrme mean field, \mathbf{W}_q the nucleonic spin-orbit mean field, and $V_q^{(K)}$ the change of the nucleonic mean fields by the K^-N interaction.

For the nucleonic part, we use the Skyrme force SLy4. For the kaonic energy-density contribution, a simple linear energy density functional is assumed as in Ref. [19],

$$\varepsilon_{KN} = -a_0 \rho_K [(1 + x_0) \rho_p + (1 - x_0) \rho_n], \quad (5)$$

where a_0 and x_0 are the K^-N interaction strength parameters. Under this assumption, the mean fields in Eqs. (3) and (4) are [19]

$$V_K = -a_0 [(1 + x_0) \rho_p + (1 - x_0) \rho_n] - V_C, \quad (6)$$

$$V_{p,n}^{(K)} = -a_0 (1 \pm x_0) \rho_K. \quad (7)$$

In the following calculations, we use a (p, n) -symmetric K^-N interaction, i.e., $x_0 = 0$ and $a_0 = 500 \text{ MeV fm}^{-3}$, which were justified as reasonable values in [19].

The pairing interaction of the nucleonic part employs a density-dependent δ pairing force [51],

$$V_q(\mathbf{r}_1, \mathbf{r}_2) = -V_0 \left[1 - \frac{\rho_N((\mathbf{r}_1 + \mathbf{r}_2)/2)}{\rho_0} \right] \delta(\mathbf{r}_1 - \mathbf{r}_2), \quad (8)$$

with the pairing strength $V_0 = 410 \text{ MeV fm}^{-3}$ for both neutrons and protons [31, 52–55] and a saturation density $\rho_0 = 0.16 \text{ fm}^{-3}$. A smooth energy cutoff is also included in the BCS calculation [55].

We assume axially-symmetric mean fields and the properties of axially-deformed nuclei are studied in cylindrical coordinates. The solutions of the SHF equation are expanded within a axially-deformed harmonic-oscillator basis [45, 48, 49].

III. RESULTS AND DISCUSSIONS

In order to study the effect of an additional K^- meson on the nucleon drip line in detail, we will examine the one-nucleon separation energies

$$S_n \equiv E[^AZ] - E[^{A-1}Z], \quad (9)$$

$$S_p \equiv E[^AZ] - E[^{A-1}(Z-1)], \quad (10)$$

which determine the drip lines and we will compare the results obtained for normal and kaonic nuclei. Also, we focus on the highest-occupied (valence) nucleon s.p. levels, which would become very weakly bound close to the drip lines. If the s.p. energy of the highest-occupied nucleon levels is still negative in the minimum of the total energy, the nucleus is supposed to exist [41].

In Fig. 1, the energies of the highest-occupied nucleon s.p. levels $-e_q$ (a), the one-nucleon separation energies S_q (b), the binding energies E (c), and the quadrupole deformations β_2 (d) of Be isotopes and their corresponding K^- nuclei are presented in comparison with the available experimental results from Ref. [56]. As indicated by the theoretical e_q and S_q values, the nuclei with $N = 2-8$ neutrons and their corresponding K^- nuclei exist. However, $^{13,17,19}\text{Be}$ ($N = 9, 13, 15$) are unbound systems due to pair breaking. Therefore, the neutron drip line locates at ^{12}Be ($N = 8$). The proton drip line reaches at ^6Be ($N = 2$). Experimentally, the nuclei from ^6Be ($N = 2$) to ^{16}Be ($N = 12$) have been observed [56], but the experimental values of S_n for ^{12}Be ($N = 8$) and S_p for ^7B ($N = 2$) are negative. Therefore, the proton and neutron drip lines locate at ^6Be ($N = 2$) and ^{12}Be ($N = 8$), respectively.

The additional K^- meson shifts down clearly the energies of the highest-occupied nucleon s.p. levels e_q (most notable for those in strongly bound inner orbits) and thus increases the total binding energies. The shift for the proton levels is larger than that for the neutron levels, even for weakly bound states, which is due to the increased Coulomb field. The decrease of quadrupole deformations, as shown in Fig. 1(d), is due to the attractive K^-N interaction [19]. With an additional K^- meson, $^{17}_{K^-}\text{Be}$ ($N = 13$) and $^{19}_{K^-}\text{Be}$ ($N = 15$) remain unbound, while $^{13}_{K^-}\text{Be}$ ($N = 9$) becomes marginally bound, but its S_n is still negative. The neutron drip line point $N = 8$ for Be isotopes is thus not shifted by an additional K^- meson. Moreover, due to the major impact on the proton levels, a bound nucleus $^5_{K^-}\text{Be}$ ($N = 1$) is found, but its one-proton separation energy S_p remains negative. An extension effect of an additional K^- meson on the proton drip line is thus found, which can be attributed to the attraction of the added Coulomb interaction between kaon and proton. A similar phenomenon was also found by additional Λ hyperons due to the attractive ΛN interaction [41].

Fig. 2 shows the preceding results for $^{11-28}\text{O}$ ($N = 3-20$) as well as the corresponding K^- nuclei. In this case all isotopes are subsphaeroidal as illustrated in panel (d). The theoretical results of the total energies are in quite good agreement with the experimental values. All isotopes from ^{12}O ($N = 4$) to ^{28}O ($N = 20$) exist with negative e_n and e_p . The separation energies S_n and S_p of all nuclei with $N = 5-16$ are posi-

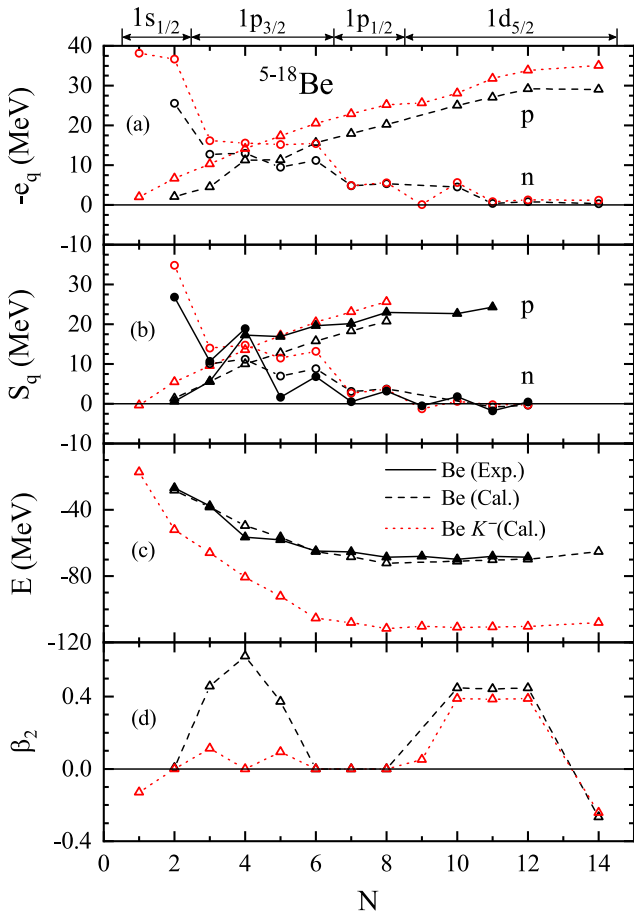


FIG. 1. (a) Energies of the highest-occupied nucleon s.p. levels $-e_q$ ($q = n, p$) (the neutron level is indicated on the top; the proton level is $1p_{3/2}$), (b) one-nucleon separation energies S_q , (c) binding energies E , (d) quadrupole deformations β_2 of Be isotopes (dashed lines) and their corresponding K^- nuclei (dotted lines), obtained with $a_0 = 500 \text{ MeV fm}^{-3}$ and $x_0 = 0$ in Eqs. (6,7). The experimental S_q and E values of normal nuclei obtained from Ref. [56] are also included for comparison (solid lines).

tive, whereas S_n becomes negative at $N = 17$ theoretically and experimentally [56], and thus the neutron drip line locates at ^{24}O ($N = 16$). The theoretical proton drip line is reached at $N = 4$ with ^{13}F being unbound, whereas experimentally it lies at $N = 5$. The experimental one-proton separation energy S_p of ^{14}F is negative.

In contrast to the results of Be isotopes in Fig. 1, the additional K^- meson increases slightly the energies of the highest-occupied neutron s.p. levels of $^{11-24}_{K^-}\text{O}$ ($N = 3-16$), but decreases those of $^{25-28}_{K^-}\text{O}$ (valence neutron levels $1d_{3/2}$). As a consequence, $^{25}_{K^-}\text{O}$ becomes unbound and the neutron removal energies of $^{27-28}_{K^-}\text{O}$ are reduced. Thus, a reducing effect of the K^- on the neutron drip line for O isotopes is found. This is an interesting result and will be analyzed in detail in the following. On the other hand, a bound $^{11}_{K^-}\text{O}$ and increasing one-proton separation energies of $^{12-24}_{K^-}\text{O}$ are found. Thus, an extension effect of K^- meson on the proton drip line is obvious.

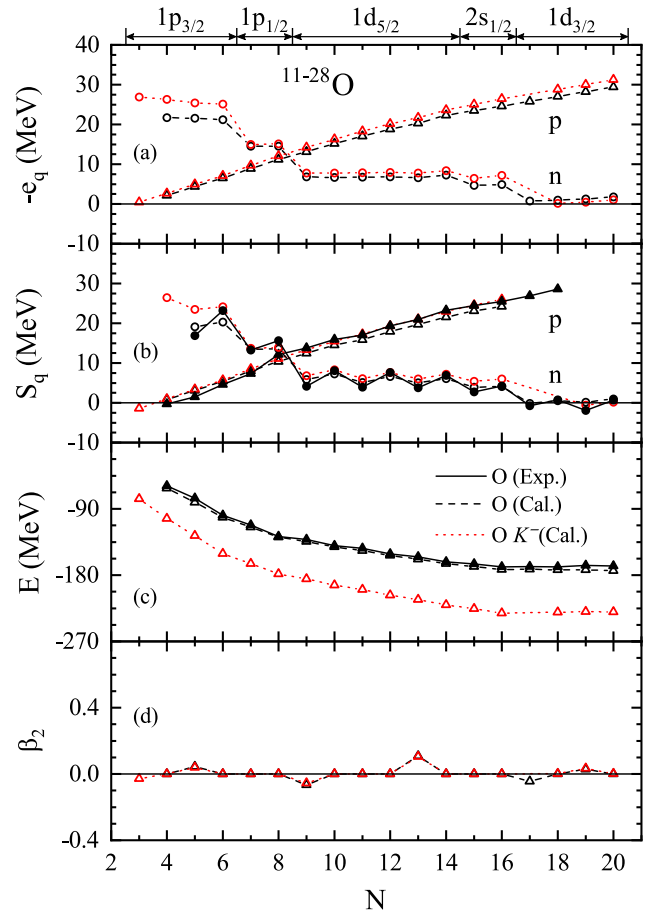


FIG. 2. Same as Fig. 1, but for O isotopes.

The same phenomenon occurs for Ne isotopes, as observed in Fig. 3. All isotopes $^{16-34}\text{Ne}$ ($N = 6-24$) exist, as experimentally [56]. $^{35,36}\text{Ne}$ are unbound systems. For $^{17-30}\text{Ne}$ ($N = 7-20$), S_n and S_p are positive both experimentally and theoretically, while S_n of ^{31}Ne ($N = 21$) is negative theoretically but marginally positive experimentally. Thus, the neutron drip line locates at ^{30}Ne ($N = 20$) theoretically and at ^{32}Ne ($N = 22$) experimentally. The proton drip line is not reached for nuclei with $N > 6$ experimentally and theoretically. A weakly bound ^{16}Ne ($Z = 10, N = 6$) and an unbound ^{15}F ($Z = 9, N = 6$) are found on the theoretical side, while the experimental S_p of ^{16}Ne is slightly negative [56].

However, $^{16}_{K^-}\text{Ne}$ with positive S_p and $^{15}_{K^-}\text{F}$ with negative S_p are bound nuclei and thus the additional K^- meson firmly establishes the proton drip line at ^{14}O for $N = 7$ nuclei, and in fact also $^{15}_{K^-}\text{Ne}$ becomes bound. All kaonic nuclei $^{15-34}_{K^-}\text{Ne}$ ($N = 5-24$) exist. Thus, the additional K^- meson does not affect the neutron drip line of Ne isotopes, although the energies of the highest-occupied neutron s.p. level ($1d_{3/2}, 1f_{7/2}$) of $^{27-32}_{K^-}\text{Ne}$ ($N = 17-22$) decrease due to the additional K^- meson. This is similar to the case of O isotopes as displayed in Fig. 2. In addition, in these larger nuclei, the deformation changes due to the kaon are much smaller than those of Be isotopes in Fig. 1(d).

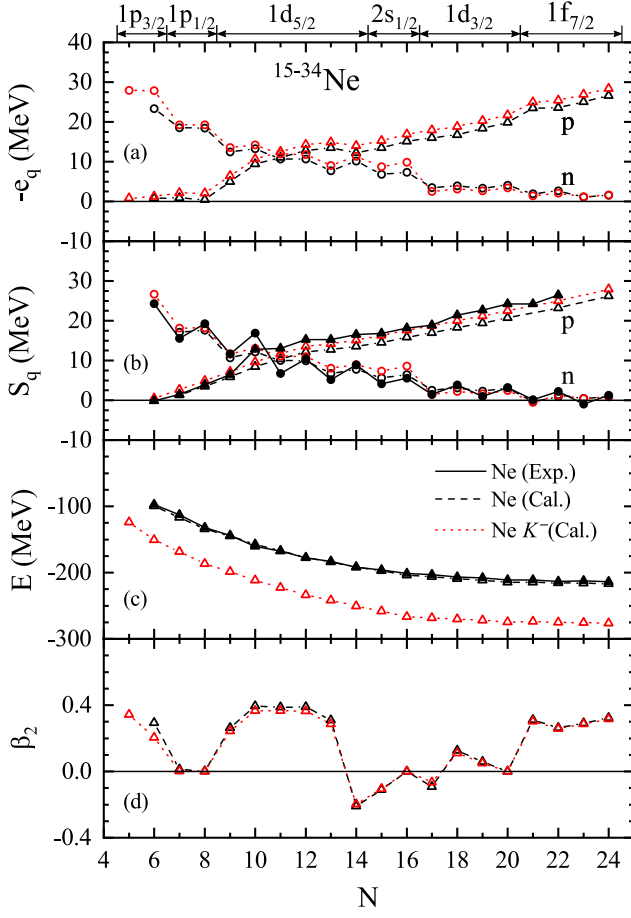


FIG. 3. Same as Fig. 1, but for Ne isotopes.

As mentioned in Sec. II, the results of K^- nuclei shown in the previous figures are obtained with the K^-N interaction strength $a_0 = 500 \text{ MeV fm}^{-3}$. Because of the uncertainty of the K^-N interaction strength, we explore the energies of the highest-occupied neutron s.p. levels of $^{27-32}_{K^-}\text{Ne}$ ($N = 17-22$) with K^-N interaction strengths $a_0 = 100, 200, \dots, 600 \text{ MeV fm}^{-3}$ in Fig. 4, respectively. It is interesting to note that the K^- meson does not always increase the energies of the highest-occupied neutron s.p. levels when increasing the K^-N interaction strength. In particular, for the weakly bound $1f_{7/2}$ levels, a weak K^-N interaction ($a_0 = 100, 200 \text{ MeV fm}^{-3}$) causes an increase of binding, whereas repulsion only sets in for $a_0 \gtrsim 300 \text{ MeV fm}^{-3}$. This will be analyzed later.

To further illustrate the above feature, we show in Fig. 5 the effect of an additional K^- meson on the neutron s.p. levels of the spherical drip-line nuclei ^8Be , ^{28}O , and ^{30}Ne with three different K^-N interaction strengths $a_0 = 100, 300, 500 \text{ MeV fm}^{-3}$, respectively. Evidently, the spin-orbit splitting of the orbitals $1p_{1/2,3/2}$ and $1d_{3/2,5/2}$ in K^- nuclei is larger than that in the corresponding normal nuclei. This effect reduces the binding of the $1d_{3/2}$ valence levels in $^{28}_{K^-}\text{O}$ and $^{30}_{K^-}\text{Ne}$. Here we remark that the level inversion between orbitals $2s_{1/2}$ and $1d_{5/2}$ in light kaonic nuclei obtained

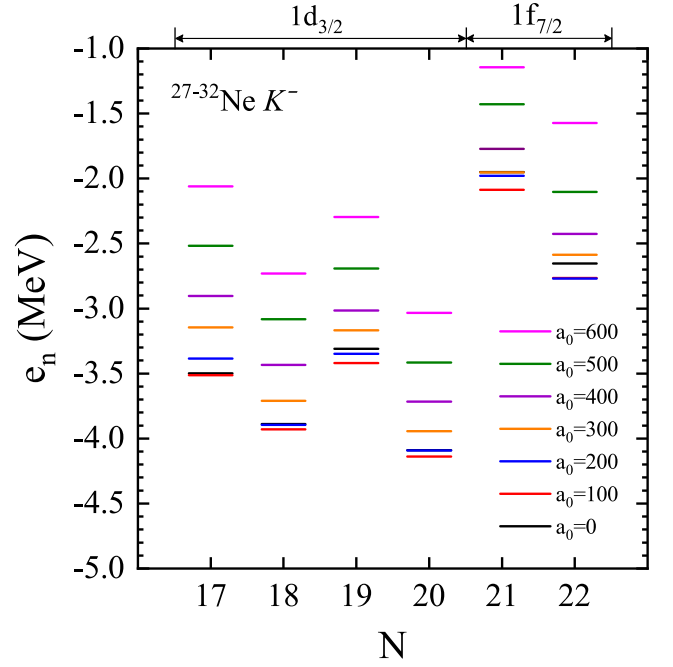


FIG. 4. Energies of the highest-occupied neutron s.p. levels of $^{27-32}_{K^-}\text{Ne}$ and their corresponding normal nuclei ($a_0 = 0$) obtained with different K^-N interaction strengths a_0 (in units of MeV fm^{-3}).

by a RMF model [57] is not found in our SHF calculations.

In order to understand the shift of the neutron s.p. levels by the addition of a kaon, we analyze the Schrödinger equation (2). One notes that both the central potential V_n and the spin-orbit potential W_n are modified when including a kaon [18, 19]. We remind that the spin-orbit potential of nucleons in the SHF approach is [44, 58]

$$W_q = \frac{W_0}{2}(\nabla\rho + \nabla\rho_q) + \frac{t_1 - t_2}{8}J_q - \frac{t_1x_1 - t_2x_2}{8}J, \quad (11)$$

with $q = n$ or p . Qualitatively, the strong K^-N attraction shrinks the nucleus. This leads to a deepening of the mean fields in the core region of the nucleus, but a weakening in the peripheral part that is essential for weakly bound valence neutrons. Moreover, there is always a delicate competition between V_n and W_n for some levels. In order to visualize these effects, we compare in Fig. 6 the potentials $V_n(r)$ and $W_n(r)$ of the drip line nuclei ^8Be , ^{28}O , and their corresponding K^- nuclei, together with the partial densities $\rho_i = 4\pi r^2 v_i^2 |\phi_i(r)|^2$ of the various occupied neutron s.p. levels. One notes that indeed the attractive K^-N interaction contracts the density distributions and thus enhances.

We note that $V_n(r)$ and $W_n(r)$ of $^{12}_{K^-}\text{Be}$ and $^{28}_{K^-}\text{O}$ are deeper than their normal nuclei for $r \lesssim 2.9 \text{ fm}$, $r \lesssim 3.0 \text{ fm}$, and $r \lesssim 3.2 \text{ fm}$, $r \lesssim 3.8 \text{ fm}$, respectively. The strongly-bound neutron levels $1p_{1/2,3/2}$, $1d_{5/2}$, and $2s_{1/2}$ of ^{28}O are concentrated well within the core region $r \lesssim 3 \text{ fm}$, which explains their gain of energy and the larger splitting of $1p_{1/2}$ and $1p_{3/2}$ in K^- nuclei, see Fig. 5. Similar phenomena can be found in ^{12}Be . On the contrary, a large amount of the $1d_{3/2,5/2}$ -state neutrons locate in the range of $3.2 - 3.8 \text{ fm}$, where the central potentials

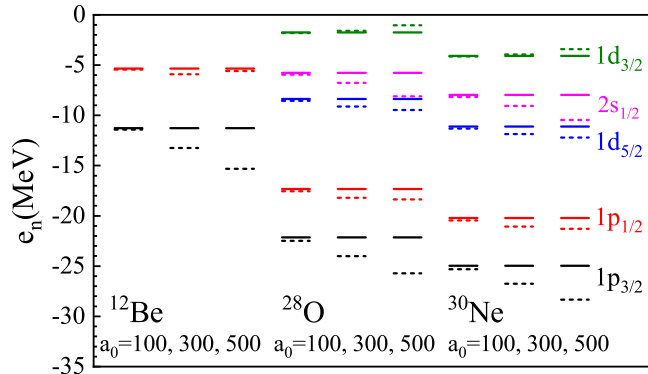


FIG. 5. Partial neutron s.p. levels of spherical nuclei ^{12}Be , ^{28}O , ^{30}Ne (solid lines) and their corresponding K^- nuclei (dashed lines) with $a_0 = 100, 300, \text{ and } 500 \text{ MeV fm}^{-3}$.

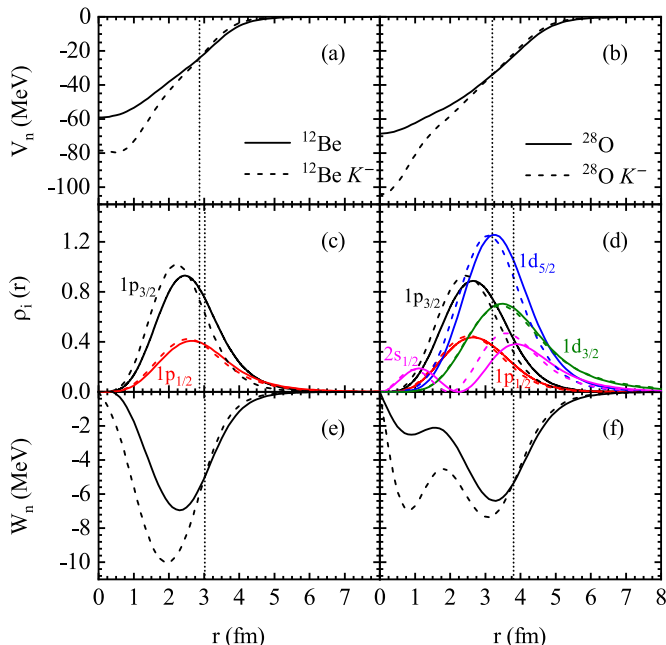


FIG. 6. The mean fields $V_n(r)$ and spin-orbit potentials $W_n(r)$, and the partial densities $\rho_i(r) = 4\pi r^2 v_i^2 |\phi_i(r)|^2$ normalized to the actual occupation numbers of all occupied neutron s.p. levels in the normal nuclei ^{12}Be and ^{28}O and their corresponding K^- nuclei with $a_0 = 500 \text{ MeV fm}^{-3}$. The vertical dotted lines label the crossings between the $V_n(r)$ and $W_n(r)$ of normal and K^- nuclei.

are smaller and the spin-orbit potentials are larger in K^- nuclei than in the normal nuclei. Therefore, the splitting of $1d_{5/2}$ and $1d_{3/2}$ is still enhanced in K^- nuclei. However, the most peripheral $1d_{3/2}$ neutrons are embedded in weaker both central and spin-orbit mean fields at $r \gtrsim 3.8 \text{ fm}$, which accounts for the upward shift of that level.

In conclusion, the effect of an additional K^- meson on the neutron drip line depends on the highest-occupied neutron s.p. level of nuclei near the neutron drip line. If this level is an orbit without spin-orbit splitting (e.g., $2s_{1/2}$) or the lower orbit

with splitting (e.g., $1p_{3/2}$ and $1d_{5/2}$), the additional K^- may extend or not shift the neutron drip line. If instead this level is an upper orbit with splitting (e.g., $1d_{3/2}$), the additional K^- can decrease its binding and reduce the neutron drip line, such as for O isotopes. This effect is caused by the shrinking of the nucleon wave functions due to a particularly strongly attractive K^-N interaction. A similar role of an additional K^- in influencing s.p. levels was pointed out in the RMF approach [57]. In addition, an extension of the proton drip line is always found due to added kaon, in particular because of its negative electric charge.

IV. SUMMARY

We explored the effect of an additional K^- meson on the neutron and proton drip lines of Be, O, and Ne isotopes using SHF approach with a simple K^-N Skyrme-type force and the nuclear SLy4 force including a pairing contribution. The single-particle levels, binding energies, and quadrupole deformations were obtained by solving the SHF equations self-consistently. Due to the attractive K^-N interaction, the additional $1s$ -state K^- meson shrinks the nucleon density distribution and increases its gradient. This increases the binding of strongly bound inner single-particle orbits, but might decrease the one of peripheral valence orbits, also by an enhanced spin-orbit splitting in the kaonic nuclei. Since the highest-occupied nucleon single-particle levels and one-nucleon separation energies determine the position of the drip line, corresponding effects were observed and analyzed in this paper.

We also remark at this point that the treatment of kaonic nuclei in the static SHF approach can only be approximate, as their lifetime is very short and an improved dynamical approach would be required for a more realistic description, including at least the imaginary parts of kaon wave function and mean field. In particular, very recently the J-PARC collaboration group measured the inclusive missing-mass spectrum of the $^{12}\text{C}(K^-, p)$ reaction and extracted the potential depth of both real and imaginary parts [59]. Thus, in the future our model can be improved by devising a more realistic kaon-nucleon Skyrme force and adding the imaginary part of the kaon optical potential, aided by current [59] and future experimental data concerning K^- nuclei. Furthermore, the mean-field approximation employed here might be inadequate in particular for light nuclei and weakly bound states, and a beyond-mean-field treatment [60–62] might be required for a more realistic modeling.

ACKNOWLEDGMENTS

This work was supported by the National Natural Science Foundation of China under Grants No. 11775081 and No. 11875134, and the Natural Science Foundation of Shanghai under Grant No. 17ZR1408900.

-
- [1] T. Kishimoto, Phys. Rev. Lett. **83**, 4701 (1999).
- [2] Y. Akaishi and T. Yamazaki, Phys. Rev. C **65**, 044005 (2002).
- [3] M. Agnello *et al.* (FINUDA Collaboration), Phys. Rev. Lett. **94**, 212303 (2005).
- [4] T. Yamazaki *et al.*, Phys. Rev. Lett. **104**, 132502 (2010).
- [5] Y. Sada *et al.* (J-PARC E15), Prog. Theor. Exp. Phys. **2016**, 051D01 (2016).
- [6] Y. Ichikawa *et al.*, JPS Conf. Proc. **8**, 021020 (2015).
- [7] A. Doté, H. Horiuchi, Y. Akaishi, and T. Yamazaki, Phys. Rev. C **70**, 044313 (2004).
- [8] T. Muto, Nucl. Phys. A **804**, 322 (2008).
- [9] A. Doté, T. Hyodo, and W. Weise, Phys. Rev. C **79**, 014003 (2009).
- [10] J. Hrtánková and J. Mareš, Phys. Rev. C **96**, 015205 (2017).
- [11] S. Maeda, Y. Akaishi, and T. Yamazaki, Proc. Jpn. Acad., Ser. B **89**, 418 (2013).
- [12] S. Marri, S. Kalantari, and J. Esmaili, Eur. Phys. J. A **52**, 361 (2016).
- [13] E. Friedman, A. Gal, J. Mareš, and A. Cieplý, Phys. Rev. C **60**, 024314 (1999).
- [14] X. H. Zhong, G. X. Peng, L. Li, and P. Z. Ning, Phys. Rev. C **74**, 034321 (2006).
- [15] D. Gazda, E. Friedman, A. Gal, and J. Mareš, Phys. Rev. C **76**, 055204 (2007).
- [16] T. Muto, T. Maruyama, and T. Tatsumi, Phys. Rev. C **79**, 035207 (2009).
- [17] R. Y. Yang, W. Z. Jiang, Q. F. Xiang, D. R. Zhang, and S. N. Wei, Eur. Phys. J. A **50**, 1 (2014).
- [18] X. R. Zhou and H.-J. Schulze, Int. J. Mod. Phys. E **22**, 1350038 (2013).
- [19] Y. Jin, C. F. Chen, X. R. Zhou, Y. Y. Cheng, and H.-J. Schulze, Prog. Theor. Exp. Phys. **2019**, 123D03 (2019).
- [20] Z. X. Liu, C. J. Xia, W. L. Lu, Y. X. Li, J. N. Hu, and T. T. Sun, Phys. Rev. C **98**, 024316 (2018).
- [21] M. T. Win and K. Hagino, Phys. Rev. C **78**, 054311 (2008).
- [22] B. N. Lu, E. G. Zhao, and S.-G. Zhou, Phys. Rev. C **84**, 014328 (2011).
- [23] B. N. Lu, E. Hiyama, H. Sagawa, and S.-G. Zhou, Phys. Rev. C **89**, 044307 (2014).
- [24] H. Mei, K. Hagino, J. M. Yao, and T. Motoba, Phys. Rev. C **90**, 064302 (2014).
- [25] W. X. Xue, J. M. Yao, K. Hagino, Z. P. Li, H. Mei, and Y. Tanimura, Phys. Rev. C **91**, 024327 (2015).
- [26] X. Y. Wu, H. Mei, J. M. Yao, and X. R. Zhou, Phys. Rev. C **95**, 034309 (2017).
- [27] J. W. Cui, X. R. Zhou, and H.-J. Schulze, Phys. Rev. C **91**, 054306 (2015).
- [28] J. W. Cui, X. R. Zhou, L. X. Guo, and H.-J. Schulze, Phys. Rev. C **95**, 024323 (2017).
- [29] W. Y. Li, J. W. Cui, and X. R. Zhou, Phys. Rev. C **97**, 034302 (2018).
- [30] A. Umeya, T. Motoba, and K. Itonaga, J. Phys.: Conf. Ser. **1643**, 012110 (2020).
- [31] B. C. Fang, W. Y. Li, C. F. Chen, J. W. Cui, X. R. Zhou, and Y. Y. Cheng, Eur. Phys. J. A **56**, 1 (2020).
- [32] T. Harada and Y. Hirabayashi, Nucl. Phys. A **759**, 143 (2005).
- [33] M. Baldo, G. F. Burgio, and H.-J. Schulze, Phys. Rev. C **58**, 3688 (1998).
- [34] T. Harada, R. Honda, and Y. Hirabayashi, Phys. Rev. C **97**, 024601 (2018).
- [35] A. Gal, E. V. Hungerford, and D. J. Millener, Rev. Mod. Phys. **88**, 035004 (2016).
- [36] E. Hiyama, Y. Yamamoto, T. Motoba, T. A. Rijken, and M. Kamimura, Phys. Rev. C **78**, 054316 (2008).
- [37] T. T. Sun, E. Hiyama, H. Sagawa, H.-J. Schulze, and J. Meng, Phys. Rev. C **94**, 064319 (2016).
- [38] J. Mareš and B. K. Jennings, Phys. Rev. C **49**, 2472 (1994).
- [39] Y. H. Tan and P. Z. Ning, Eur. Phys. J. A **20**, 257 (2004).
- [40] Y. Jin, X. R. Zhou, Y. Y. Cheng, and H.-J. Schulze, Eur. Phys. J. A **56**, 1 (2020).
- [41] X. R. Zhou, A. Polls, H.-J. Schulze, and I. Vidaña, Phys. Rev. C **78**, 054306 (2008).
- [42] C. Samanta, P. R. Chowdhury, and D. N. Basu, J. Phys. G: Nucl. Part. Phys. **35**, 065101 (2008).
- [43] E. Khan, J. Margueron, F. Gulminelli, and A. R. Raduta, Phys. Rev. C **92**, 044313 (2015).
- [44] D. Vautherin and D. M. Brink, Phys. Rev. C **5**, 626 (1972).
- [45] D. Vautherin, Phys. Rev. C **7**, 296 (1973).
- [46] M. Rayet, Nucl. Phys. A **367**, 381 (1981).
- [47] M. Rayet, Ann. Phys. **102**, 226 (1976).
- [48] M. Bender, P. H. Heenen, and P. G. Reinhard, Rev. Mod. Phys. **75**, 121 (2003).
- [49] J. R. Stone and P. G. Reinhard, Prog. Part. Nucl. Phys. **58**, 587 (2007).
- [50] H.-J. Schulze and E. Hiyama, Phys. Rev. C **90**, 047301 (2014).
- [51] N. Tajima, P. Bonche, H. Flocard, P. H. Heenen, and M. Weiss, Nucl. Phys. A **551**, 434 (1993).
- [52] M. T. Win, K. Hagino, and T. Koike, Phys. Rev. C **83**, 014301 (2011).
- [53] H. Sagawa, X. R. Zhou, X. Z. Zhang, and T. Suzuki, Phys. Rev. C **70**, 054316 (2004).
- [54] H. Sagawa, X. R. Zhou, and X. Z. Zhang, Phys. Rev. C **72**, 054311 (2005).
- [55] M. Bender, K. Rutz, P. G. Reinhard, and J. A. Maruhn, Eur. Phys. J. A **8**, 59 (2000).
- [56] <https://www.nndc.bnl.gov/nudat2/>.
- [57] R. Y. Yang, W. Z. Jiang, and S. N. Wei, Phys. Lett. B **795**, 188 (2019).
- [58] E. Chabanat, P. Bonche, P. Haensel, J. Meyer, and R. Schaeffer, Nucl. Phys. A **635**, 231 (1998).
- [59] Y. Ichikawa *et al.*, Prog. Theor. Exp. Phys. **2020**, 123D01 (2020).
- [60] J. W. Cui, X. R. Zhou, L. X. Guo, and H.-J. Schulze, Phys. Rev. C **95**, 024323 (2017).
- [61] W. Y. Li, J. W. Cui, and X. R. Zhou, Phys. Rev. C **97**, 034302 (2018).
- [62] H. Mei, K. Hagino, J. M. Yao, and T. Motoba, Phys. Rev. C **97**, 064318 (2018).